

IRONMAN: GNN-assisted Design Space Exploration in High-Level Synthesis via Reinforcement Learning

Nan Wu

nanwu@ucsb.edu
University of California, Santa Barbara
Santa Barbara, CA, USA

Yuan Xie

yuanxie@ucsb.edu
University of California, Santa Barbara
Santa Barbara, CA, USA

Cong Hao

callie.hao@ece.gatech.edu
Georgia Institute of Technology
Atlanta, GA, USA

ABSTRACT

Despite the great success of High-Level Synthesis (HLS) tools, we observe several unresolved challenges: 1) the high-level abstraction of programming styles in HLS sometimes conceals optimization opportunities; 2) existing HLS tools do not provide flexible trade-off (Pareto) solutions among different objectives and constraints; 3) the actual quality of the resulting RTL designs is hard to predict. To address these challenges, we propose an end-to-end framework, namely **IronMan**, in this work. The primary goal is to enable a flexible and automated design space exploration (DSE), to provide either optimal solutions under user-specified constraints, or various trade-offs among different objectives (such as different types of resources, area, and latency). Such design space exploration either requires tedious manual efforts or is not achievable to attain these goals through existing HLS tools. There are three components in **IronMan**: 1) **GPP**, a highly accurate graph-neural-network-based performance and resource predictor; 2) **RLMD**, a reinforcement-learning-based multi-objective DSE engine that explores the optimal resource allocation strategy, to provide Pareto solutions between different objectives; 3) **CT**, a code transformer to assist **RLMD** and **GPP**, which extracts the data flow graph from original HLS C/C++ and automatically generates synthesizable code with HLS directives. The experimental results show that, 1) **GPP** achieves high prediction accuracy, reducing prediction errors of HLS tools by 10.9× in resource utilization and 5.7× in timing; 2) **RLMD** obtains optimal or Pareto solutions that outperform the genetic algorithm and simulated annealing by 12.7% and 12.9%, respectively; 3) **IronMan** is able to find optimized solutions perfectly matching various DSP constraints, with 2.54× fewer DSPs and up to 6× shorter latency than those of HLS tools. **IronMan** is also up to 400× faster than the heuristic algorithms and HLS tools.

1 INTRODUCTION

High-Level Synthesis (HLS) benefits the ASIC and FPGA design automation by enabling automated transformation from behavioral description in high-level languages (C/C++, etc.) to RTL-level designs. Besides widely used commercial HLS tools for FPGA [17] and ASIC [1], a great amount of recent effort focuses on improving RTL design quality such as loop transformation and memory allocation [2, 21], performance and/or resource prediction [8, 18, 19], and the design space exploration (DSE) [12], etc.

Even though the previous effort shows great effectiveness, there are several principal challenges unaddressed. 1) The high-level abstraction of programming styles in HLS, such as loops and function calls, sometimes performs poorly for hardware implementation, and conceals further optimization opportunities [7]. To overcome this problem, Licht JD *et al.* [7] propose a toolbox, from which

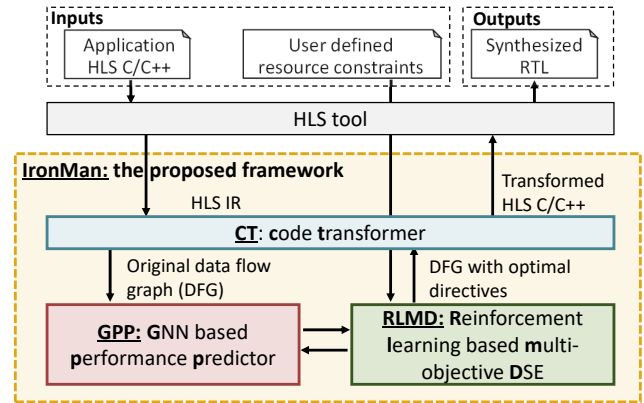


Figure 1: The overall framework, **IRONMAN, is integrated of **CT**, **GPP**, and **RLMD**. **GPP** is a highly accurate graph-neural-network-based performance and resource predictor; **RLMD** is a reinforcement-learning-based multi-objective DSE engine for resource allocation; **CT** is a code transformer that extracts the data flow graph from original HLS C/C++ and generates synthesizable code with new HLS directives.**

developers can choose multiple classes of transformations with different objectives such as increasing parallelism. Even provided with transformation tools, manual efforts for exploration are still needed. 2) Existing DSE approaches as well as commercial HLS tools do not provide flexible trade-off (Pareto) solutions between different objectives and constraints (e.g., latency and resource usage, or different types of resources). As pointed out by Schafer *et al.* [12], existing approaches usually sacrifice design latency for less resource, or vice versa. However, one alternative is to trade one type of resource for another (e.g., LUT and DSP in FPGA) while maintaining the latency, which is unexplored and only can be done through tedious manual efforts (Detailed examples will be provided in Section 2). 3) The real quality of the resulting RTL designs is hard to predict, especially for irregular data paths. As most existing predictors are model-based (e.g., COMBA [18]), they are more suitable for well-structured data flows such as perfect or semi-perfect loops. Another approach is applying machine learning for predictions [3, 8, 19], which often requires to extract abundant features after design synthesis and/or implementation.

In this work, we propose an end-to-end framework, namely **IRONMAN**, to address the aforementioned challenges. There are two major goals in this framework: 1) to enable a flexible and automated DSE, aiming to *explore various trade-offs between different*

objectives such as resource types and latency, which is not achievable through existing HLS tools or DSE engines. 2) to provide an accurate RTL design performance predictor, which *does not require any additional features* besides the original data flow graph (DFG), supporting both regular and irregular data paths. Fig. 1 illustrates the overall flow of **IRONMAN**, composed of three components that seamlessly cooperate with each other. We briefly introduce the components and summarize our contributions as follows.

- **GPP**: we propose a highly accurate Graph neural network (GNN) based performance predictor of HLS designs (for both regular and irregular data paths), including resource utilization (DSPs and LUTs) and critical path (CP) timing. Notably, it predicts the *actual performance* after physical synthesis (placement and routing) rather than the *synthesized* results by HLS tools. Moreover, GPP can generalize to previously unseen DFGs.
- **RLMD**: we propose a deep reinforcement learning based multi-objective design space exploration engine for resource allocation in HLS. Assisted by **GPP**, **RLMD** explores the optimal resource allocation strategy based on user-specified constraints. The objectives include minimizing resource utilization, optimizing critical path timing and/or minimizing DFG computation latency. **RLMD** also provides Pareto solutions between different objectives that are unavailable in HLS tools.
- **CT**: we propose a code transformer, which extracts the DFGs from original HLS C/C++ and re-generates synthesizable code with HLS directives after **RLMD** applies DSE to obtain optimal directives. **CT** reveals *concealed optimization opportunities* for achieving higher parallelism and shorter latency, and allows *flexible and finer-grained DSE* under user-specified constraints.
- **IRONMAN**: while each proposed component alone can independently contribute to the HLS community (performance prediction, DSE, code transformation), we integrate them into a framework, **IRONMAN**, and demonstrate the end-to-end benefits on benchmarks from real-world applications.
- The experimental results show that, 1) **GPP** achieves high prediction accuracy in *actual* resource, reducing prediction errors of HLS tools by 10.9× in resource utilization and 5.7× in critical path timing; 2) **RLMD** obtains optimal or Pareto solutions that outperform the generic algorithm and simulated annealing by 12.7% and 12.9%, respectively; 3) on real-case benchmarks, **IRONMAN** is able to find solutions satisfying various DSP constraints, with 2.54× fewer DSPs and up to 6× shorter latency than those of HLS tools, while being up to 400× faster than the heuristic algorithms and HLS tools.

2 MOTIVATION

HLS tools have been extensively studied for years with great achievements alleviating the hardware design burdens. There are many important investigations focusing on the optimization of HLS tools, performance predictions, and DSE technologies [3, 7, 8, 12, 18–20]. Regardless of these achievements, however, we have the following observations that reveal insufficiency of the existing HLS tools.

1. Higher level abstractions in HLS can obstruct optimization opportunities. (1) The irregular logic, cascaded and/or imperfect loops in HLS coding usually require manual or complicated

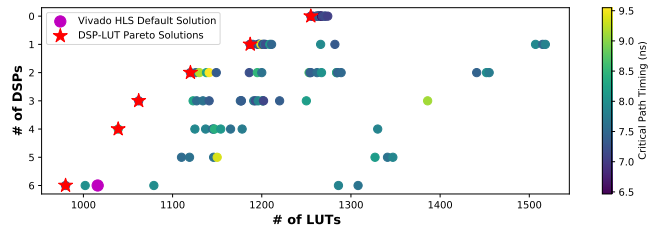


Figure 2: Pareto solutions between DSPs and LUTs on a FPGA. The default HLS solution is not on the Pareto frontier, and it is non-trivial to obtain the Pareto solutions in a large design space.

Orig. Code: for (int i=0; i<8; i++) sum += a[i]*b[i];					
	Method	Cycles	DSP	LUTs	CP (ns)
1	Original	17	1	75	4.07
2	unroll (factor=8, complete)	2	8	100	5.04
3	unroll (factor=4)	4	4	87	4.83
4	unroll (factor=3)	8	3	109	7.44
5	unroll + allocation (limit=3) *	4	6	168	8.76
6	Code Transform (CT)	2	8	100	5.03
7	CT + allocation (limit=2)	5	3	196	9.91
8	CT + allocation (limit=3)	4	6	168	8.54
9	▷ CT + resource (5 Mul_LUT)	2	2	1742	4.24
10	▷ CT + resource (4 Mul_LUT)	2	2	1741	4.01
11	▷ CT + resource (3 Mul_LUT)	2	3	1461	3.98

* HLS pragmas do not always behave as expected.

Table 1: Approaches to meeting DSP constraints (e.g., ≤ 3) of the above *for_loop*, with different clock cycles (latency), numbers of LUTs, and critical path (CP) timing. This work explores *CT + resource* approaches.

code transformations to improve performance [7]. (2) The structured HLS coding style hinders advanced or fined-grained performance and resource optimization. Table 1 demonstrates a simple multiplication-accumulation function using a for-loop. To explore the trade-offs between the DSP usage and the number of clock cycles (latency), the typical ways are to use *unroll* pragmas or manual loop-tiling, such as line 1-4. However, when the loop boundary (e.g., 8) is not divisible by the DSP constraint (e.g., 3), it results in a *partial unrolling* as line 4, introducing undesired latency increment (from 4 to 8) and worsening the critical path (CP) timing (from 5ns to 7.4ns). The nested loops further complicate this problem and make it much harder to balance between latency and resource (imagine a 5-layer nested loop with a DSP constraint of 17). Motivated by the necessity of *better performance and more flexible optimization choices*, we propose a **code transformer (CT)**, which breaks up the high-level abstractions and their boundaries, fuses them into a new data flow graph (DFG), and re-generates synthesizable C/C++ code with pragmas. An example of CT is given in Fig. 3 (a). CT easily allows to use directives, such as *allocation* and *resource* pragmas, to conduct finer-grained DSEs for resource and performance, as shown in Table 1 from line 7-11. Notably, using **CT+resource** approaches proposed in this work (line 9-11) achieves best latency

(i.e., 2) within the DSP constraint (i.e., ≤ 3) without manual efforts. An alternative to constrain DSP is to use `#pragma HLS allocation instance=mul` but at the cost of increased latency (line 5-8).

2. HLS tools do not always provide the best solution, nor automatically provide trade-offs (Pareto solutions). Given a DFG, either original or generated by CT, it requires an extensive DSE to explore the fine-grained trade-offs among performance, resource usage, and resource type (e.g. DSPs v.s. LUTs). Fig. 2 exemplifies the Pareto solutions between LUTs and DSPs, achieved by specifying that certain multiplications use LUTs instead of DSPs. The red stars are the Pareto solutions and the magenta dot is the single HLS default solution. The input DFG has 200 operations and is synthesized by Vivado HLS and implemented by Vivado. In this example, first, the HLS default solution is not on the Pareto frontier; second, it demonstrates a large design space for finding the Pareto solutions, and thus the **DSE for Pareto solutions is non-trivial**. Worth noting, the solution space grows exponentially even for a binary selection between DSP and LUT for each multiplication, and the different data precision (bit-width) further complicates this problem. Motivated by the necessity and difficulty of a *flexible and fine-grained DSE*, we propose a deep reinforcement learning based DSE tool, **RLMD**.

3. Existing HLS performance predictors and DSE tools do not support irregular logic and data paths. Instead, they mostly target highly regular data paths, e.g., perfect and nested loops with high-level directives such as pipelining and array partition [18, 20]. As such, these analytical model based predictors and high level DSE tools are *not suitable for irregular logic and data paths* (especially for timing estimation). Fortunately, the inherent graph structure of DFGs provides a promising opportunity to exploit the representative power of GNNs [4, 6, 11]. Motivated by the necessity of *DSE and high-accuracy prediction for irregular data path* and the *intrinsic graph structure of DFGs*, we propose a GNN-based HLS performance predictor, **GPP**, **enabling RLMD for DSE on arbitrary DFGs**.

3 OVERALL FRAMEWORK

The overall framework of IRONMAN is shown in Fig. 1. The inputs to IRONMAN are HLS C/C++ code and user-specified constraints. The outputs are re-generated multi-objective-optimized code with proper HLS directives, either meeting the user-specified constraints (e.g., resource or latency), or providing Pareto solutions between different optimization objectives.

① **CT** extracts the intrinsic DFGs from the intermediate representation (IR) of HLS tools to release more optimization opportunities, and then re-generates synthesizable C/C++ code with optimized DFGs. An example of how CT re-generates C++ code is shown in Fig. 3 (a), with the extracted DFG in (b). Each intermediate operator may have various bit-width, e.g., $\langle 12 \rangle$ means a 12-bit data precision.

② **GPP**, a **GNN-based performance predictor**, estimates *actual* resource usage after physical synthesis of the DFGs. GNNs [4, 6, 11] are adopted for three reasons. (1) DFGs are graphs, which are naturally suitable for GNNs to learn the underlying information from graph structures. (2) DFGs vary in topologies and sizes, and in order to generalize predictions to new or unseen graphs,

Original Code:

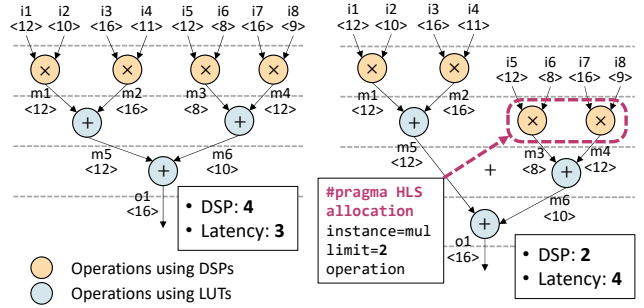
```
for (int i=0; i<4; i++) sum += a[i] * b[i];
```

Transformed Code with `resource` pragma

```
TYPE1 m1 = i1 * i2;    TYPE2 m2 = i3 * i4;
TYPE3 m3 = i5 * i6;    TYPE4 m4 = i7 * i8;
TYPE5 m5 = m1 + m2;    TYPE6 m6 = m3 + m4;
TYPE7 m7 = m5 + m6;
#pragma HLS resource variable = m3 core = Mul_LUT
```

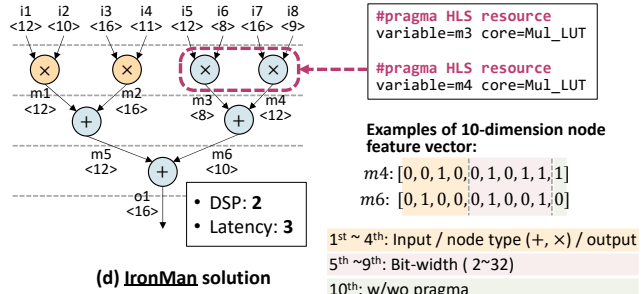
* The `TYPE` can be varied data precisions (bit-width), which further expands the design space (e.g., from INT2 to INT32).

(a) Code Transformation (CT)



(b) HLS default solution

(c) HLS solution with constraints



(d) IRONMAN solution

```
#pragma HLS resource
variable=m3 core=Mul_LUT
#pragma HLS resource
variable=m4 core=Mul_LUT
```

Examples of 10-dimension node feature vector:
m4: [0, 0, 1, 0, 0, 1, 0, 1, 1, 1]
m6: [0, 1, 0, 0, 0, 1, 0, 0, 1, 0]

1st ~ 4th: Input / node type (+, x) / output
5th ~ 9th: Bit-width (2~32)
10th: w/wo pragma

Figure 3: An example of IRONMAN solution. (a) The original HLS code and transformed code with resource pragma, indicating the importance of CT for IRONMAN solutions. (b) HLS default solution with 4 DSPs and a latency of 3; (c) HLS solution with naive constraints, with 2 DSPs while increasing latency from 3 to 4; (d) IRONMAN solution, with 2 DSPs and an unchanged latency of 3.

it is necessary to use *inductive GNNs* [4] to learn fixed-size *graph embeddings*. (3) IRONMAN runs inferences of trained GNN models during execution, which is orders of magnitude faster than running HLS tools.

③ **RLMD**, an **RL-based DSE engine**, takes the DFG, its corresponding graph embedding, and user-specified constraints as inputs, to make endeavors for optimal resource allocation strategy. RL is adopted for two main reasons. (1) The design space grows exponentially with the size of DFGs, different graph topologies, and various data precision. Whereas an RL agent can explore design space proactively and learn from past experiences, and a well pre-trained agent can generalize to new problems by minimal fine-tuning efforts. (2) By carefully defining reward functions, RL agents can achieve multi-objective optimization automatically, getting rid

of manual efforts to craft useful heuristics. Noteworthy, an informative and well-crafted state representation will significantly benefit the learning process in RL problems, motivating the integration of GPP and RLMD, where the graph embeddings are naturally suitable for state representation in this problem. Consequently, the graph embeddings enable RLMD to generalize across different DFG topologies, and GPP largely accelerates the training process of RLMD by quick evaluations of solutions generated by RLMD.

As a case study of IRONMAN, the specific problem solved is **to find a resource allocation solution that strictly meets the DSP constraint, or to find Pareto solutions between DSPs and LUTs on FPGAs, without sacrificing DFG computation latency**. For simplicity, the DFGs only have additions and multiplications, where RLMD decides whether to assign the directive `#pragma HLS resource core=Mul_LUT` to each multiplication operation, to minimize LUTs within DSP constraints. As shown in Fig. 3, (b) is the default Vivado HLS solution with 4 DSPs and a latency of 3; (c) is a naive solution using `#pragma HLS allocation instance=mul limit=2` to enforce two DSPs, resulting in an increased latency from 3 to 4; (d) shows the solution of IRONMAN with 2 DSPs and an unchanged latency of 3, using `#pragma HLS resource variable=(var) core=Mul_LUT`. Notably, such a finer-grained DSE of IRONMAN is enabled by CT.

4 PROPOSED GPP AND RLMD

Since GPP provides inputs and performance predictions of RLMD, we first introduce the structure of GPP, and then discuss the detailed formulation of RLMD.

4.1 GPP

The key role of a GNN is to extract adequate information of node types, graph topology and connectivity within a large DFG, and encode the information into low-dimensional vector representations that can be used for either downstream tasks or high-accuracy performance prediction.

Node Feature Vector. In a DFG, each node is encoded into a 10-dimension node feature vector, as the example shown in Fig. 3(d). The 1st to 4th dimension use one-hot representations to encode the node types, including input nodes, intermediate nodes/operations (additions and multiplications), and output nodes. The 5st to 9th dimension encode the data precision of an intermediate operation, which in this work ranges from INT2 to INT32. We use a binary representation to encode the precision minus one, so the bit-width can be expressed in 5 bits. The 10th dimension indicates whether an HLS directive `#pragma HLS resource` is applied to this node. Note that such an encoding scheme can be easily extended to support more types of nodes/operations or pragmas.

Graph Embedding. We employ three GNN models to separately predict the number of utilized LUTs, DSPs, and CP timing. The three models have the same structure, as illustrated in the left part of Fig. 4. For each GNN model, the inputs are adjacency matrices and node feature matrices of DFGs. The first two layers are graph convolutional [6], with 64 and 128 units respectively and ReLu activations. In each graph convolutional layer, the node embedding is updated by aggregating feature vectors from its neighbors, and one node can receive information from farther nodes by

stacking multiple layers. Next, the learned node embeddings are summarized by a mean pooling to create a graph representation, denoted by a 128×1 vector. This representation vector is then passed to a feed-forward network with three fully connected layers and leaky ReLu ($\alpha = 0.1$) activations to generate a graph embedding, denoted by a 64×1 vector. The last layer is the output of the GNN, including a single unit with ReLu activation to provide the prediction result.

Integration with RLMD. To integrate with RLMD, we combine the three embedding vectors that focus on different characteristics of DFGs into one graph embedding, shown as the 192×1 vector in Fig. 4. Finally, the graph embedding vector is concatenated with the meta data of the input DFG, and passed to RLMD as its inputs. The DFG meta data include the size of the DFG (i.e., the number of input/intermediate/output nodes and the number of edges) and the number of multiplications in this DFG. Given predictions of LUT/DSP/CP, solutions generated by RLMD can be quickly evaluated, providing feedback to further improve the policy of RLMD.

4.2 RLMD

RL Formulation. The resource allocation problem in HLS, as a typical RL [13] problem, can be formulated as a Markov Decision Process (MDP), with four key components.

- States: the set of possible states. In this problem, a state can be every possible partially assigned DFGs.
- Actions: the set of eligible actions under a state. In this problem, given the current state and the currently considered node of the DFG, the available action is whether to assign a certain directive to this node.
- State transition: given a state and an action, the probability distribution of next states.
- Reward: the immediate reward of taking an action in a state. In this problem, the reward is 0 for all intermediate actions, with an exception for the last action where the reward is the evaluation of the fully assigned DFG subject to user-specified constraints.

Specifically, the state at time step t is defined as s_t , which is a concatenation of features including a 192×1 graph embedding vector that describes the current status of the DFG, the ID of current node to assign a directive, metadata of the DFG, and the DSP constraint (either user-specified or automatically generated for Pareto solution exploration). The action a_t is a valid assignment of a directive to the t^{th} node, i.e., whether to use LUTs for multiplication computation on this node. We define the reward r_t as a negative weighted sum of predicted LUTs, CP timing, and the difference between predicted and targeted DSPs, as follows:

$$r_t = \begin{cases} -\alpha LUT_p - \beta |DSP_{target} - DSP_p| - \lambda CP_p, & t = T \\ 0, & 0 < t < T \end{cases}. \quad (1)$$

where α , β and λ are hyper-parameters.

At the initial state s_0 , all the multiplication nodes in a DFG are unassigned. At each time step t , the RL agent observes the current state s_t , takes an action a_t , receives a reward r_{t+1} and arrives at a new state s_{t+1} . The nodes are assigned with directives sequentially based on their node IDs. Given T multiplication nodes in total, the

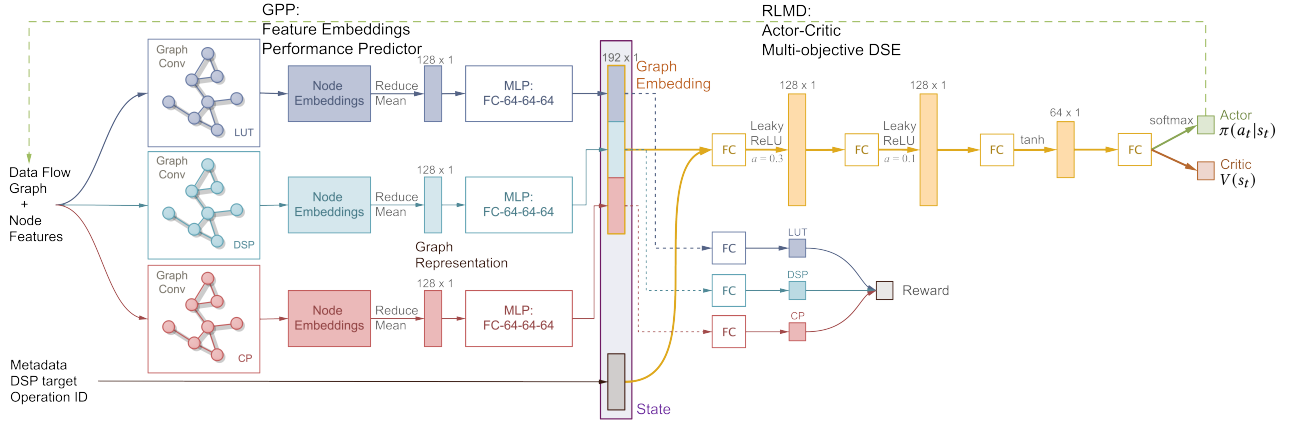


Figure 4: GPP and RLMD structure. GPP encodes information of the DFG adjacency and node features, to make predictions of LUT/DSP/CP. Concatenating the graph embedding provided by GPP with the meta data of the input DFG, RLMD then outputs a binary probability distribution $\pi(a_t|s_t)$ of whether to use LUTs for multiplication computation on the current node, and a scalar as the state-value function.

final state s_T corresponds to a DFG completely assigned with proper directives. The goal is to maximize the expected rewards received.

RLMD Training. We adopt the actor-critic method with Monte-Carlo learning [13]: the actor aims to learn an optimal policy $\pi_\theta(a_t|s_t)$ parameterized by θ , which is a probability distribution of valid actions under the current state; the critic approximates the state-value function $V(s_t) = \mathbb{E}_\pi[\sum_{k=0}^{T-t} \gamma^k r_{t+k}|s_t]$ by parameters w , which is an estimate of total rewards starting from state s_t to s_T following policy π , measuring the goodness of this state. The $\gamma \in (0, 1]$ is the discount factor. As shown in the right part of Fig. 4, there are shared parameters in the actor π_θ and the critic V_w , and for clarity we denote θ and w separately. By Monte-Carlo learning, the parameters are updated once only after one complete episode (i.e., one complete assignment process of a DFG), leading to the updates as follows:

$$\delta_i = \gamma^{T-i} r_T - V_w(s_i), \quad (2)$$

$$\Delta w \propto \sum_{i=1}^T \delta_i \nabla_w V_w(s_i), \quad (3)$$

$$\Delta \theta \propto \sum_{i=1}^T \delta_i \nabla_\theta \log \pi_\theta(a_i|s_i), \quad (4)$$

where T is the total time steps in one episode. Through repeated episodes (i.e., sequences of states, actions, and rewards), the actor learns optimized policy that will maximize cumulative rewards.

Our ultimate goal is to enable RLMD to generate higher-quality results and transfer knowledge across various DFGs as it gains experience from predicting resource allocation strategies on more and more DFGs. Thus, we formally formulate the overall optimization objective function as:

$$\mathcal{J}(\theta, w, G) = \frac{1}{K} \sum_{g \in G} \mathbb{E}_{g,l \sim \pi_\theta} [R_{g,l}], \quad (5)$$

where $\mathcal{J}(\theta, w, G)$ measures the total expected rewards over all training DFGs. The DFG dataset G has K different DFGs, each of which is denoted as g . $R_{g,l}$ is the episode reward (i.e., r_T defined in Eq.(1)) under the resource allocation solution l on the DFG g . To get better exploration during training, we apply ϵ -greedy algorithm for action selections [13].

RLMD Fine-tuning. Given an unseen DFG, the simplest way is to directly apply the pre-trained RLMD for inference, which can generate a solution within a second. When higher quality solutions are expected, the pre-trained RLMD can be further finetuned on this particular DFG with the help of by GPP. The fine-tuning step provides the flexibility to trade off between a quick solution using the pre-trained RLMD (which has learned rich knowledge of resource allocation strategies on other DFGs) and a longer yet better one for a particular DFG.

5 EXPERIMENT

5.1 Experiment Setup

Dataset Generation. In order to train GPP and RLMD, we build a dataset containing both synthetic and real-case DFGs, which are generated by our CT. We randomly create 47 different synthetic DFGs, each of which has 100 to 200 operations of either multiplication or addition. Each operation has two operands with random data precision between INT2 and INT16. On each DFG, we further generate up to 100 sets of directives, which specify a subset of multiplications to be implemented by LUTs rather than DSPs. For real-case DFGs, we consider 8 benchmarks from MachSuite [10], CHStone [5] and PolyBench/C [9]: *gemm*, *kernel_2mm*, *kernel_durbin* (small, large), *spmv*, *stencil3d* (small, large), and *kernel_adi*. The ground-truth (actual) resource usage (LUT/DSP) and critical path timing are synthesized by Vivado HLS [17] and implemented by Vivado [15] targeting Xilinx Ultra96 part xc7z020c1g484.

Training Process. To demonstrate the generalization capability of IRONMAN across different DFGs and applications, GPP and RLMD are trained on part of DFGs from the dataset and evaluated on rest

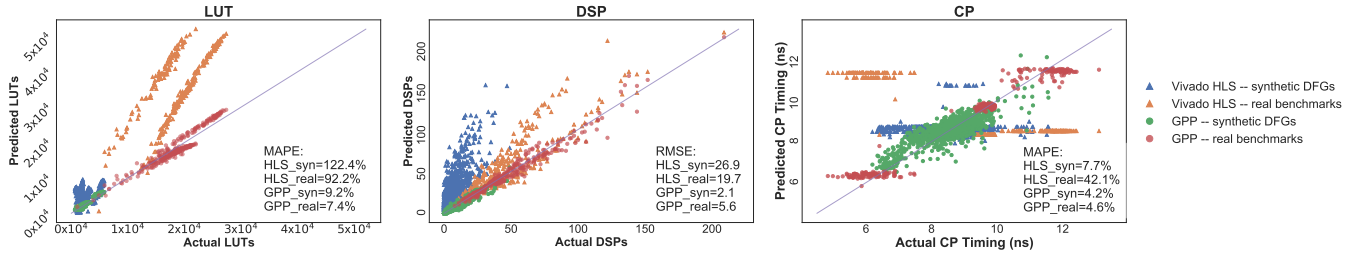


Figure 5: GPP predictions on resource utilization (LUTs and DSPs), and critical path timing (CP timing).

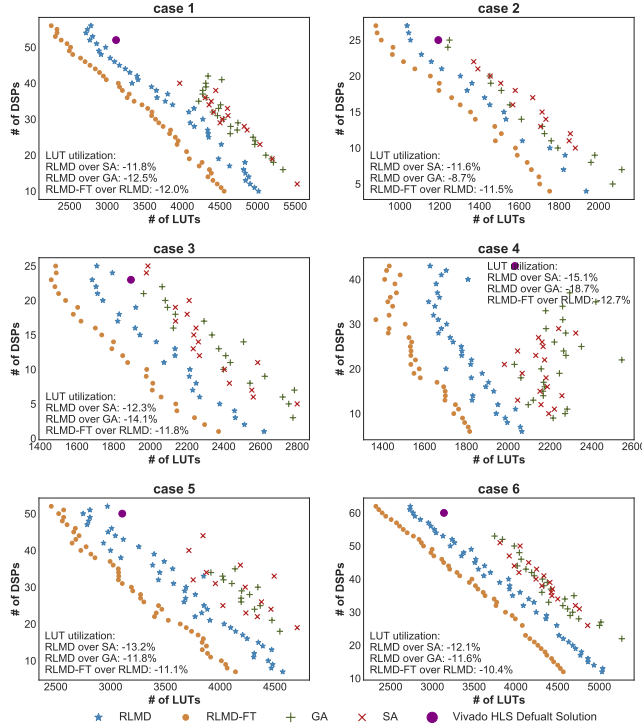


Figure 6: Pareto solutions found by RLMD, SA and GA on synthetic DFGs, with unchanged latency.

of them, where 41 different synthetic DFGs and 4 real-case DFGs (*kernel_durbin* and *stencil3d*) compose the training set.

GPP is trained via regression to minimize the mean squared logarithmic errors for DSPs and CP timing, and the mean absolute errors for LUTs, respectively. The supervised learning process and GNN models enable GPP to identify features and necessary information to generalize performance prediction and graph embeddings across different DFGs. In terms of hyper-parameter selection, the GPP is trained over 200 epochs with batchsize as 32. The Adam optimizer is applied with an initial learning rate of 0.01 decaying exponentially.

Once GPP is trained, it is integrated with RLMD and the training process of RLMD can be started. To train RLMD, we provide tuples in the form of $[DFG_{index}, DSP_{target}]$ to the RL agent, and the optimization goal is to maximize the average cumulative rewards on all of the tuples, so that the agent can learn resource allocation

strategies under different DSP constraints and across different DFGs. There have 1125 different tuples in total, and each tuple appears 8 times during the training process, amounting to 9,000 episodes. As far as fine-tuning the RLMD on a particular DFG, we additionally conduct 500 episodes of training with various targeted DSPs. The parameters in RLMD are also learned by Adam optimizer with the learning rate of 0.008. We empirically set the discount rate $\gamma = 0.95$, and the exploration rate $\epsilon = 0.08$ decaying exponentially. In the reward function, we have $\alpha = 0.002$, $\beta = 5$, and $\lambda = 0.1$.

5.2 Evaluation

Baselines. To evaluate GPP, we compare with the HLS tool Vivado HLS [17] and the machine learning based circuit performance predictor Pyramid [8]. To evaluate IRONMAN, we compare with three optimization methods: 1) genetic algorithm [16] (denoted by GA), one prominent instance of evolutionary optimization algorithms; 2) simulated annealing [14] (denoted by SA), an effective technique to approximate the global optima in an extremely large search space; 3) Vivado HLS, the default solutions provided by the Vivado HLS tool [17]. Solutions from different optimization methods are finally synthesized and implemented by Vivado to derive the actual performance. Worth noting, none of the state-of-the-art DSE methods for HLS [12] can do fine-grained resource allocation as we proposed in this work, because of the code transformation we proposed.

GPP vs. HLS tool and Pyramid [8]. GPP is evaluated on both synthetic DFGs and real-case DFGs. Fig. 5 compares GPP predictions with HLS synthesis reports regarding LUT, DSP and critical path timing. For LUT utilization, the mean absolute percentage errors (MAPEs) of GPP on synthetic and real-case DFGs are 7.4% and 9.2%, respectively, whereas the MAPEs of Vivado HLS are 122.4% and 92.2%, respectively. For DSP utilization, the prediction accuracy is measured by root-mean-square error (RMSE) since MAPE is not applicable when the ground truth appears to be zero. GPP achieves 5.6 and 2.1 in RMSE for synthetic and real-case DFGs, while Vivado HLS reaches 26.9 and 19.7, respectively. For critical path timing, the MAPEs of GPP are 4.2% and 4.6% on synthetic and real-case DFGs, whereas the MAPEs of Vivado HLS are 7.7% and 42.1%. On average, GPP reduces the prediction error of Vivado HLS by 10.9 \times in resource and 5.7 \times in timing.

Pyramid [8] is also an ML-based framework for resource and timing prediction. The major difference between GPP and Pyramid is the features required for predictions. Pyramid needs 72 features from HLS reports as inputs, which enforce the running of HLS to get VHDL designs, possibly consuming hours for large designs;

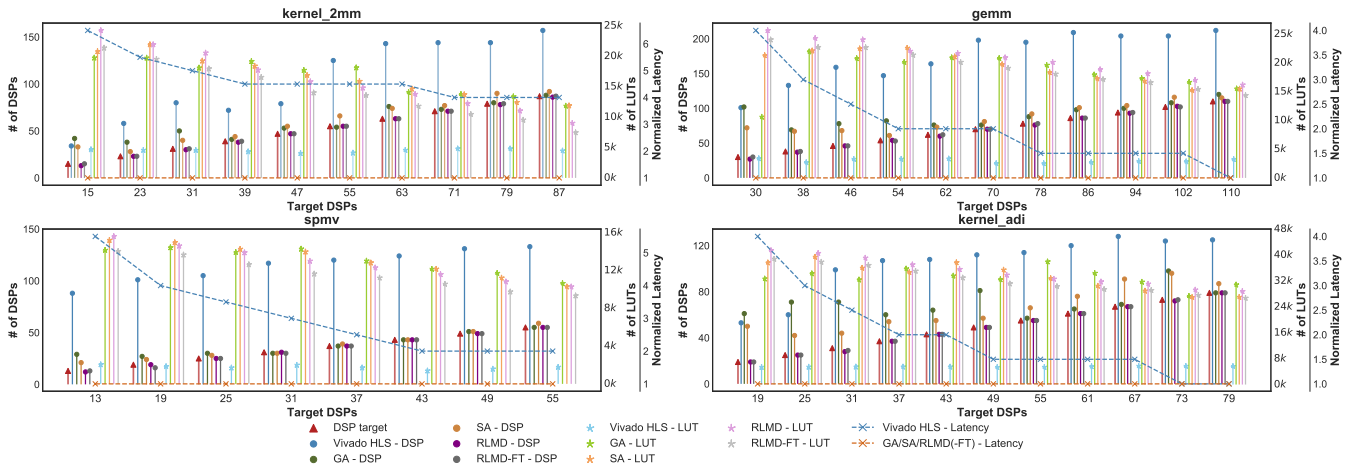


Figure 7: IRONMAN performance on real-case benchmarks. IRONMAN meets DSP constraints for 39 out of 40 cases, and meets all 40 after fine-tuning, while SA, GA and Vivado HLS meet for 2, 6, and 0 cases, respectively. With 1.3 \times and 1.44 \times less DSP usage, IRONMAN after fine-tuning uses 7.7% and 5.9% less LUTs than SA and GA, respectively. Meanwhile, IRONMAN always maintains the shortest latency while Vivado HLS increases the latency by up to 6 \times .

whereas GPP can make high-accuracy predictions simply from raw DFGs (within a second). Pyramid considers four ML models and an ensemble of these four, none of which includes graphical structure. The reported results show that the averaged prediction error of a single ML model is 17.8% for resource and 17.3% for timing, with the ensemble reaching 5.5% for resource and 4.1% for timing.

RLMD vs. GA and SA. Fig. 6 compares RLMD with GA and SA regarding the Pareto solutions between LUTs and DSPs. Obviously, RLMD outperforms GA and SA by a large margin. Given the same number of DSPs, RLMD is capable to find solutions reducing the LUT utilization by 12.7% and 12.9%, compared with SA and GA, respectively. After performing fine-tuning, additional 11.6% reduction in LUT utilization is achieved.

These promising results show great potentials of applying RL for DSE in HLS. Through trials and interactions with GPP and user-specified constraints, RLMD is able to gradually understand which directive should be assigned to which node, and proactively learn proper resource allocation strategies by balanced exploration and exploitation. In contrast, one underlying assumption in GA is that the offspring of two strong individuals among a population is often stronger, which is not the case in DSE for HLS problems, thus reducing its effectiveness. Similarly, SA is a probabilistic technique and uses meta-heuristic aiming to approximate the global optima, which ignores past experiences and searches solutions to some extent hinging on randomness, thus not always reliable.

IRONMAN vs. All. As depicted in Fig. 7, IRONMAN is fully evaluated by comparing with SA, GA and Vivado HLS on four real-case benchmarks, *kernel_2mm*, *gemm*, *spmv*, and *kernel_adi*, whose sizes are 2 – 4 \times larger than synthetic DFGs. To showcase IRONMAN capable to perfectly satisfy user specifications without sacrificing latency, we specify different DSP constraints within 20% to 80% of the maximal number of DSPs for each case.

Among four real-case benchmarks with 40 different DSP constraints in total, IRONMAN is able to meet 39 (97.5%) of them, and

can further improve to 40 (100%) by fine-tuning. Whereas SA, GA and Vivado HLS only meet the constraints for 2 (5%), 6 (15%) and 0 cases, respectively. Specifically, IRONMAN on average consumes 98.5% of the targeted DSPs (improved to 99.3% with fine-tuning), whereas those found by SA, GA and Vivado HLS use 1.29 \times , 1.43 \times , and 2.54 \times more DSPs than the target, respectively. Not only can IRONMAN meet user-specified constraints much more accurately than its counterparts and HLS tools, but it always maintains the shortest latency whereas Vivado HLS results in an increased latency by up to 6 \times .

It is noteworthy that reducing DSPs without sacrificing latency is achieved at the cost of increased LUT usage. The reason for doing so is that DSP resource is usually more critical in FPGAs while LUT resource is more adequate. By perfectly satisfying DSP constraints (with 1.3 \times and 1.44 \times fewer DSPs), IRONMAN slightly increases the LUT usage by 1.2% and 3.0%, compared with SA and GA; with further fine-tuning, IRONMAN achieves additional 8.9% LUT reduction, resulting in 7.7% and 5.9% lower LUT usage than SA and GA.

Execution Time. During inference, i.e., being applied on real applications, IRONMAN only takes a few seconds (up to 10s) to get resource allocation decisions, as well as an accurate resource and timing prediction. On the other hand, Vivado HLS takes tens of minutes to synthesis the C++ code, and takes up to hours to get the exact resource usage after implementation, which is extremely time consuming especially for large applications. The SA and GA also take hours in average, because they struggle to exactly or closely meet the DSP constraint, and cannot generalize across different DFGs or DSP constraints. Since the fine-tuning for RL agent is to provide the flexibility to balance between a quick solution using the pre-trained model and a longer yet better one for a particular DFG, it is optional, and the number of episodes for fine-tuning is adjustable based on users' requirements.

6 CONCLUSION

IRONMAN is an end-to-end framework, aiming to help HLS tools generate higher quality solutions under user-specified constraints, or perform more flexible DSEs to provide Pareto solutions that are not currently supported by HLS tools. IRONMAN is equipped with a GNN-based performance predictor GPP, an RL-based DSE engine RLMD, and a code transformer. Independently, GPP achieves high prediction accuracy, reducing prediction errors of HLS tools by 5.7× in timing and 10.9× in resource; RLMD obtains Pareto solutions that outperform the GA and SA by 12.7% and 12.9%. Integrated, IRONMAN is capable to find optimized solutions perfectly matching various DSP constraints, with 2.54× fewer DSPs and up to 6× shorter latency than those of HLS tools. IRONMAN is also up to 400× faster than the heuristic algorithms and HLS tools.

REFERENCES

- [1] Cadance. Accessed: 2021-02-14. Cadance Stratus High-Level Synthesis. https://www.cadence.com/en_US/home/tools/digital-design-and-signoff/synthesis/stratus-high-level-synthesis.html.
- [2] Jason Cong et al. 2012. Optimizing memory hierarchy allocation with loop transformations for high-level synthesis. In *49th DAC*.
- [3] Steve Dai et al. 2018. Fast and accurate estimation of quality of results in high-level synthesis with machine learning. In *FCCM*.
- [4] Will Hamilton et al. 2017. Inductive representation learning on large graphs. In *NeurIPS*.
- [5] Yuko Hara et al. 2009. Proposal and quantitative analysis of the CHStone benchmark program suite for practical C-based high-level synthesis. *JIP* 17 (2009), 242–254.
- [6] Thomas N Kipf and Max Welling. 2017. Semi-supervised classification with graph convolutional networks. *ICLR* (2017).
- [7] Johannes de Fine Licht et al. 2018. Transformations of High-Level Synthesis Codes for High-Performance Computing. *arXiv:1805.08288* (2018).
- [8] Hosein Mohammadi Makrani et al. 2019. Pyramid: Machine Learning Framework to Estimate the Optimal Timing and Resource Usage of a High-Level Synthesis Design. In *29th FPL*.
- [9] Louis-Noël Pouchet and Tomofumi Yuki. 2016. PolyBench/C - the Polyhedral Benchmark suite. <http://web.cs.ucla.edu/~pouchet/software/polybench/>.
- [10] Brandon Reagen et al. 2014. MachSuite: Benchmarks for Accelerator Design and Customized Architectures. In *IISWC*.
- [11] Franco Scarselli, Marco Gori, Ah Chung Tsoi, Markus Hagenbuchner, and Gabriele Monfardini. 2008. The graph neural network model. *IEEE Transactions on Neural Networks* 20, 1 (2008), 61–80.
- [12] Benjamin Carrion Schafer and Zi Wang. 2019. High-level synthesis design space exploration: Past, present and future. *IEEE TCAD* (2019).
- [13] Richard S Sutton and Andrew G Barto. 2018. *Reinforcement learning: An introduction*. MIT press.
- [14] Peter JM Van Laarhoven and Emile HL Aarts. 1987. Simulated annealing. In *Simulated annealing: Theory and applications*. Springer, 7–15.
- [15] Vivado. Accessed: 2021-02-14. *Vivado Design Suite - HLx Editions*. <https://www.xilinx.com/products/design-tools/vivado.html>.
- [16] Darrell Whitley. 1994. A genetic algorithm tutorial. *Statistics and computing* 4, 2 (1994), 65–85.
- [17] Xilinx. Accessed: 2021-02-14. *Xilinx Vivado High-Level Synthesis*. <https://www.xilinx.com/products/design-tools/vivado/integration/esl-design.html>.
- [18] Jieru Zhao et al. 2017. COMBA: A comprehensive model-based analysis framework for high level synthesis of real applications. In *ICCAD*.
- [19] Jieru Zhao et al. 2019. Machine learning based routing congestion prediction in fpga high-level synthesis. In *DATE*.
- [20] Guanwen Zhong et al. 2016. Lin-analyzer: a high-level performance analysis tool for FPGA-based accelerators. In *53rd DAC*.
- [21] Wei Zuo et al. 2013. Improving high level synthesis optimization opportunity through polyhedral transformations. In *FPGA*.